

# A NOVEL ANFIS CONTROLLER BASED V-G ENABLED IN BIDIRECTIONAL EV CHARGER FOR REACTIVE POWER COMPENSATION

**Jangam Susmitha<sup>1</sup>, B.Parasuram<sup>2</sup>**

<sup>1</sup>*M.Tech Student, Dept.of EEE, Bheema Institute of Technology & Sciences, Adoni, Andhra Pradesh, India.*

<sup>2</sup>*Associate Professor, Dept.of EEE, Bheema Institute of Technology & Sciences, Adoni, Andhra Pradesh, India.*

## **Abstract:**

As a charger (G2V) and power generator (V2G), the ANFIS controller-based EV charger in off-board EV we propose in this research will also serve as a reactive power compensation device. In the front end, an AC-DC spiralled H-bridge transformer regulates power flow between both the grid as well as the EV battery, whereas a back-end DC-DC transformer controls this same power flow. The charger setup offers galvanic isolation from the rest of the system at the user's end as a safety precaution. The suggested ANFIS management algorithm follows active power instructions for G2V and V2G operation, as well as reactive power orders from the utility grid, as required, by controlling EV current and battery current. In addition, an adaptive notch filter-based controller is built for phase estimation and produced reference current synchronisation. The suggested control approach eliminates the phase-locked loop (PLL) from the controller design. Because the controller's steady-state and transient performance increases, its computing complexity reduces. A MATLAB/Simulink model of a 12.6 kVA off-board charge is also developed, and the proposed control individual's performance is assessed during in the EV charger's G2V, V2G, & power factor correction operations.

**Keywords:** Adaptive notch filter, Bidirectional EV Charger, Grid to vehicle, Reactive power compensation, Vehicle to grid

## **1.INTRODUCTION**

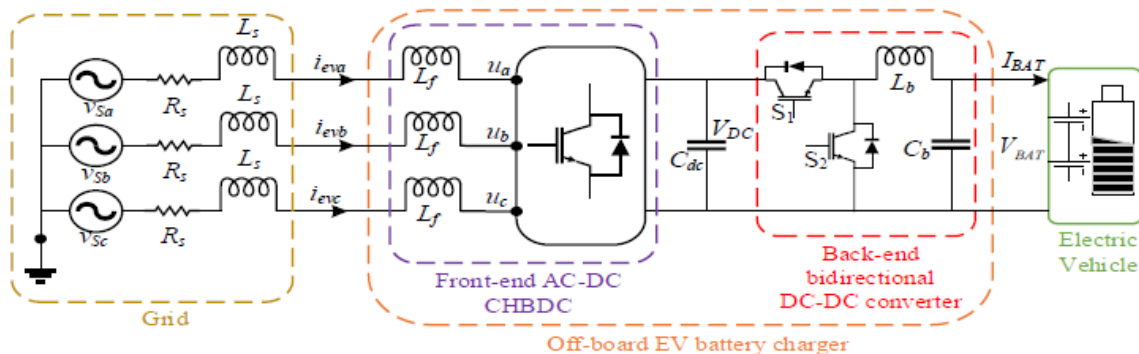
Electric-powered vehicles (EVs) have recently gained a lot of interest in developed nations because of their reduced gasoline usage and ozone-depleting chemical outflows. Off-board rapid charging facilities are an increasingly important factor in the future development of the EV market. Digital devices may be powered either in one or two directions by an external charger [2], [3]. G2V (framework to automotive) and G2L (car to lattice) are two examples of bidirectional activities that depict the flow of dynamic strength (V2G). In the smart network, the V2G activity is exciting because of the stored power of the EV batteries [3] and [4]. Degradation of Battery systems during V2G activity is just a concern, regardless of the fact that the EV batteries may be able to meet the capacity requirements of the grid. A voltage controller and other subordinate administrations like responsive energy remuneration, network-consistent pay and power problem revision may be achieved without the use of EV batteries with honeycomb shield battery length while charging. Off-board chargers are more helpful than on-board chargers for these supplementary administrations since they are more adjusted to pressure levels [6]. Power is used to deliver the responsive current in an ordinary electrical framework. For this reason the lengthy transmission and distribution agency suffers more misfortunes, which in turn reduces the overall framework productivity. The framework's voltage nature is weakened further by further voltage loss at line reactance. Thus, it is much appreciated if domestic burden requests may be responded to quickly. Aside from that, household appliances like refrigerators, clothes washers, microwaves, and many more use responsive electricity from the infrastructure, even when their owners don't pay enough. A bidirectional EV charger, on the other hand, may provide local responsive power without the requirement of additional VAR compensators. This study focuses on the pastime of EV chargers aiding the network. Off-board blaming stations of

mounted public auxiliary capabilities at neglected public areas, such as retail facilities, preventing regions, workplaces and private buildings and cafes, enable the use of electric vehicles.

The planned EV charger in [7] is designed to provide the grid with responsive power recompense. DC connect voltage is managed by EV batteries to provide uninterrupted receptive strength pay, regardless of how long they last. Furthermore, it goes beyond the extreme charging and discharging cycles that shorten battery life. Reactive energy recompense for the charger's G2V and V2G hobby isn't usually considered. To function as a receptive electrical guide, the charger is also used in [8] and [9]. However, manipulating DC voltage with EV batteries has a negative impact on their appearance and lifespan. In [10], [11], the responsive energy pay interest of the EV charger is introduced. Despite this, the suggested charger control method directs the DC join by using the EV batteries and responsive energy interest with V2G is not mentioned. [12] proposes an EV battery charger with a variety of responsive energy remuneration capabilities. However, it does not take into account the charger's interest in running at the same time in two different modes at the same time.

## 2. PROPOSED SYSTEM

For an unidirectional off-board EV rechargeable battery, a special control approach has been developed to provide rapid power compensation when referred to it from the grid. Additionally, the suggested charger regulator (ANFIS) enables the responsive electricity pay while operating the charger G2V or V2G. This study identifies the charger's responsive strength remuneration way as the automobile for framework (V4G) operating mode. A galvanic confinement feature of the proposed charger geometries makes the EV charger very dependable in everyday usage. During charging, the EV charge regulator ensures that the UPF (unity strength problem factor) is not violated. A flexible indent channel (ANF) is used for network synchronisation in the suggested charger control calculation. As a result, the regulator has added new components and simplified the execution process. Aside from that, the manipulator circle makes use of an instant electricity management system to provide a rapid response to pressure order adjustments. ANF, rather than PLL, improves the charger's ability to perform consistently throughout the country. The DC join voltage management period is given to assist the DC interface voltage in returning to its reference value in the internal current manipulation circle.



### 2.1 PROPOSED SYSTEM CONFIGURATION

#### 2.1 BIDIRECTIONAL OFF-BOARD EV BATTERY CHARGER

Fig. 1 depicts the arrangement about off EV battery charger. In order to verify the charger's responsive power compensation capabilities and the G2V or V2G operating method, a new EV charger was designed. There is just a single invigorated input power converter in the network facing front-crease AC-DC flowing H-span bidirectional (CHBDC). Lattice facing converter circuit diagram Fig. 2 shows the detailed circuit configuration of the converter. The converter's additional association has three H-span modules that are all the same level. A single level toroidal middle converter is essential to any H-span yield. The auxiliary coils of three transformer are connected in a series, which ensures that the effective operational power of each transformer matches the stage yield voltage of the other

transformers. See Fig. 2 for a visual representation of how 33.33 percent of the level voltage is contributed by each individual H-span. However, its software just at result stop enhances its presentation as opposed to typical transformer-based entirely models, where toroidal transformers are seen as a high frequency connection in the front converter [13]. The converter may operate with a single DC excitation voltage thanks to the toroidal intermediate transformer. The increased use of voltage matching sensors predicted to keep up with the equivalent energy appropriation of certain modules [13] is also eliminated [16]. [17]. More advantages include very low charging current waves; current and voltage manipulation capabilities; and galvanic confinement [13]. [12] The L-channel in Fig. 1 connects the CHBDC frame to the power grid, allowing the converter output voltage to be further broadened. Since it has a staggered design, the L-channel is capable of eliminating a higher-request substitute song. Electric vehicle (EV) batteries are priced and released with the use of a reduced back-charge DC converter (BBDC). Figure 1 shows the BBDC factor as a result of the point circuit arrangement. The two switches may be used to swap between the two different modes (Buck and Boost) (S1, S2). Controlling S2 enables the BBDC to function as a currency converter and lift mode. Consequently, the BBDC may be used in buck and lift mode to accomplish charging and discharging of the EV batteries.

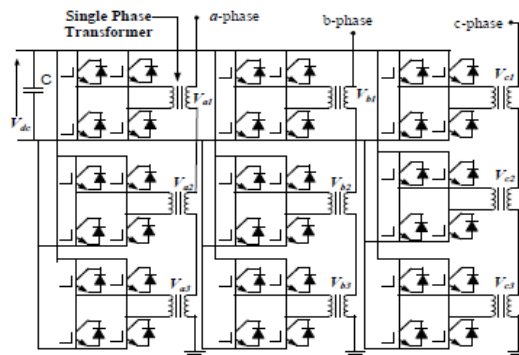


Fig. 2. CHBDC Circuit configuration

## 2.2 CONTROL STRATEGY OF THE EV CHARGER

It is intended to charge the EV battery by using dynamic power from the grid (G2V) and to ship lower back voltage levels when cited from of the lattice, i.e. V2G activity, for which the regulator deliberated in this work acts as a major purpose. It also includes the network's receptive potential when referred to by the framework's administrative user interface (UI). Figure 3 depicts the regulator form for the element. ANF is used to keep the network and charger in sync with the suggested management computation. To begin, the ANF supporting framework synchronisation is shown in [14]. Despite its independence from the framework, the ANF has been able to effectively eliminate typical PLL from the structure regulator. The ANF's strong scenarios, as described in [14], are listed below:

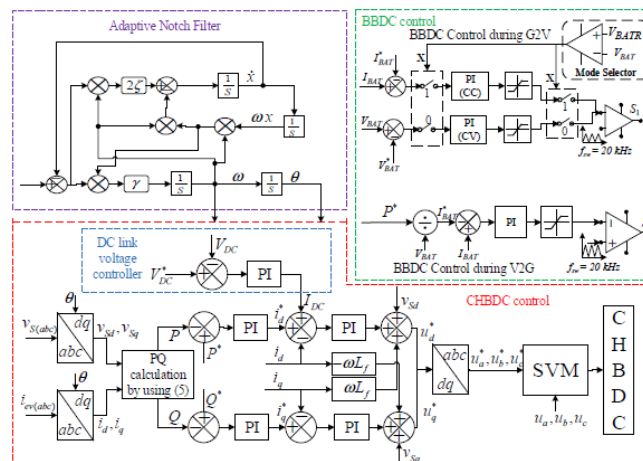


Fig. 3 Bidirectional EV charger controller block diagram

$$\begin{aligned} \ddot{x} + \omega^2 x &= 2\zeta\omega e(t) \\ \dot{\omega} &= -\gamma x \omega e(t) \\ e(t) &= u(t) - \dot{x} \end{aligned} \quad (1)$$

Information signal  $u(t)$ , repetition rate, and two real constants and are used in this equation. The ANF's speed and assessment accuracy are determined by the desire and. The ANF includes a special occasional circle at [14] for recurrence of the fundamental portion  $w_1$  with abundance  $U_1$ :

$$\begin{pmatrix} x \\ \dot{x} \\ \omega \end{pmatrix} = \begin{pmatrix} -\frac{U_1}{\omega_1} \cos(\omega_1 t + \varphi_1) \\ U_1 \sin(\omega_1 t + \varphi_1) \\ \omega_1 \end{pmatrix} \quad (2)$$

Factor ANF structure is shown in Figure 3 in order to measure a-level framework voltages  $V_{sa}$  recurrence and level factor. As part of a park exchange, the 3-stage communal voltages and flows are transferred toward the d - q from abc-define (3).

$$\begin{bmatrix} v_{sd} \\ v_{sq} \end{bmatrix} = [T] \begin{bmatrix} v_{sa} \\ v_{sb} \\ v_{sc} \end{bmatrix} \quad (3)$$

where,

$$[T] = \sqrt{\frac{2}{3}} \begin{bmatrix} \sin\theta & \sin(\theta - 2\pi/3) & \sin(\theta + 2\pi/3) \\ \cos\theta & \cos(\theta - 2\pi/3) & \cos(\theta + 2\pi/3) \end{bmatrix}$$

Change lattice  $[T]$  may be used to determine the three-stage source current's dq-outline change (3).

$$\begin{bmatrix} i_{sd} \\ i_{sq} \end{bmatrix} = [T] \begin{bmatrix} i_{sa} \\ i_{sb} \\ i_{sc} \end{bmatrix} \quad (4)$$

With this, the prompt dynamic and reactive power can assess by use (3) and (4).

$$\begin{aligned} P &= 3/2(v_{sd}i_d + v_{sq}i_q) \\ Q &= 3/2(v_{sq}i_d - v_{sd}i_q) \end{aligned} \quad (5)$$

According to Fig. 3, the intended dynamic & receptive energy is evaluated in (5), while the error signal is sent via the PI regulator to measure reference dynamic modern ( $I_d$ ) and responsive modern ( $I_q$ ) as shown in Fig. Three, as shown in the table. To charge or transport batteries, the P specifies the organization's efficiency order to be used. When charging, the charger is interested in attracting power from the lattice, and when discharging, it is interested in discharging power from a battery. The Q refers to the amount of receptive energy detected by the internet from the charger through the Q sign. Positive Q refers to the network's inductive receptive strength, which means that the charger is getting responsive power from the network. The term "negative Q" refers to the charger's resources' responsiveness to the framework, as measured by the community's capacitive receptive strength. To create the absolute dynamically contemporary component, the DC input voltage regulator yield => is included. It was then possible to contrast and shift the purposeful lattice modern to a dq-define using reference dynamic and versatile flows (4). CHBDC's reference voltage is the sum of the inward PI control circle yield and the evaluating anticipated lattice voltage within the dq-define.

A. Vehicle to Grid (G2V) In the G2V pastime approach, the charger uses the strength lattice to draw the dynamic charging energy needed to recharge the battery. In order to charge batteries, this study uses the CV/CC method, which uses a constant voltage and constant current. It is necessary to maintain consistent current flow in order to charge the reference battery to the permitted voltage stage

established by the manufacturer while maintaining a suitable strength level of reference battery charging current. Starting from that point on, the battery charge progresses at the highest possible level of voltage, with decreasing current, until it reaches its assessed removed level and the battery charge reaches its maximum possible level. Observing the higher percentage order P and keeping up with UPF's comments, the CHBDC control works in this way. The receptive electrical order Q is 0 in this manner of operation. By managing the swapping of S1 to regulate the battery charge current (DEF) and voltage, the BBDC acts as a buck - boost converter during charging ( GDEF ). Fig 3 depicts the G2V regulator generation of BBDC at a certain point. As seen in Fig 1, all pieces are identical.

B. Using a vehicle to connect (V2G) By positioning the reference energy order P to be bad regarded and Q=0, the EV charger communicates an 1800 level change between EV contemporary and lattice voltage to the battery. Using the expected electricity (standard energy P and the time stretch), the EV charger manipulates calculations to construct the reference current day. It's possible to estimate the current state of the reference battery (DEF ') by using scenario 19 without regard to the EV charger's shortcomings. Put the software grid in standby mode. At the point when the EV is connected to the framework, the charger's G2V capacity is crucial. However, with the supervision of a BBDC, power may be transferred between the heads for a short period of time. As the utility grid's needs change, so does the flow of power from of the battery to the framework. In this state, the CHBDC is maintained to function properly.

$$I_{BAT}^* = \frac{P^*}{V_{BAT}} \quad (8)$$

### **Adaptive Network based Fuzzy Inference System:**

Analyzing capacity estimate challenges using a brain network method, this adaptive neuro fuzzy system (ANFIS) is data-driven. It is common for information-driven techniques for the integration of ANFIS networks to use mathematical examples to approximate the elusive capacity. ANFIS networks have been successfully used in reserve undertakings, rule-based way management, layout recognition, and comparative concerns since its presentation. When it comes to producing fuzzy norms from a record yield informative index, the bushy model provided by Takagi and Sugeno and Kang is included in this framework.

#### **2.2.1. ANFIS structure**

The bushy induction architecture is significantly more broad in that it is possible to have two sources of information and one outcome. The bushy in the case of Takagi & Sugeno's concepts is carried by the modern basis as follows:

z is f if x and y are A and B, respectively (x,y)

$z = f(x, y)$  is a dazzling ability in the subsequent, where A & B are indeed the bushy unit in the predecessors and  $z = A$  quadratic for the two information elements, x and y, is the norm. The outcome of the framework may be shown in the fuzzy region as specified by the predecessor using any other ability. A zero request is made if  $f(x,y)$  is a constant function. Each general next is chosen by a fuzzily singleton in Sugeno's fuzzy induction framework, which is presumably seen as a be beyond of Mamdani's fuzzy induction framework. On the off chance that  $f(x,y)$  is regarded to be a first demand polynomial, a main request Sugeno Fuzzy model is constructed. A first demand rule Sugeno fuzzy deduction framework may represent the two needs as:

**Rule 1: If x is A1 and y is B1 then  $f1 = p1x + q1y + r1$**

**Rule 2: If x is A2 and y is B2 then  $f2 = p2x + q2y + r2$**

Takagi and Sugeno devised a type-three fuzzy derivation framework, which is used here. Every trend, in this enticing structure, produces an instantaneous combination of the information items provided over a regular time period. The weighted normal of each preferred's end result is the ultimate end result. Figure 4.5 shows a comparison of equal ANFIS shapes.

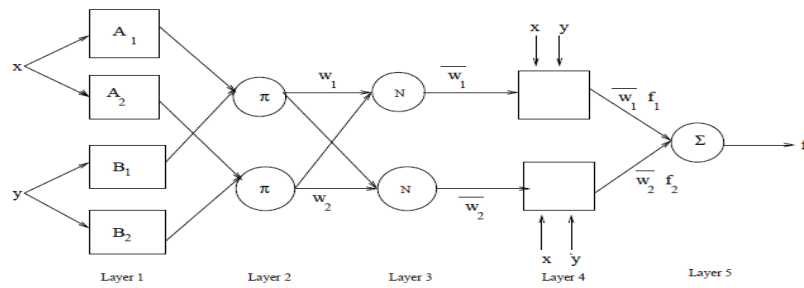
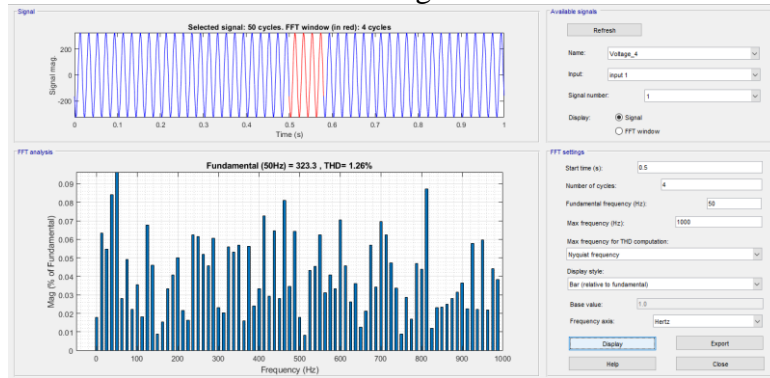
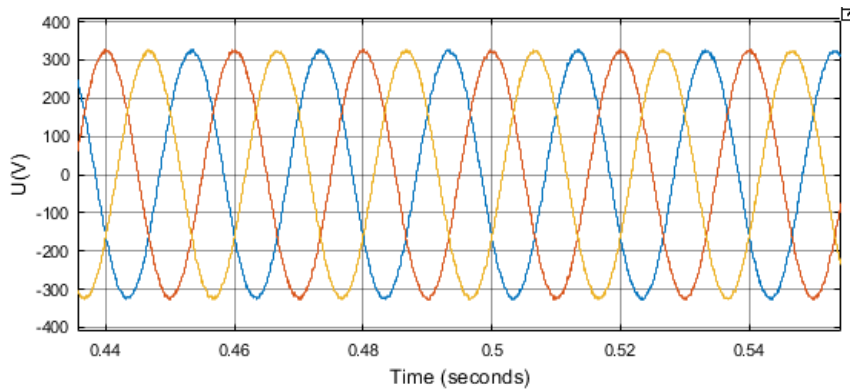
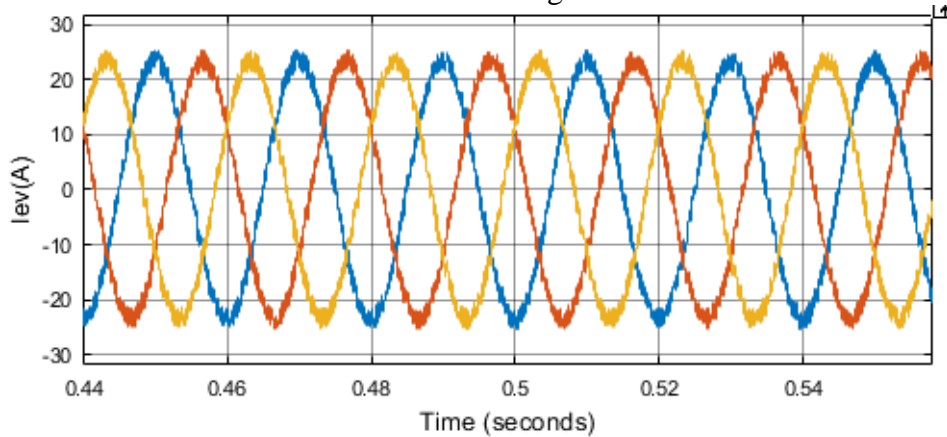


Fig.4.5. Type-3 ANFIS Structure

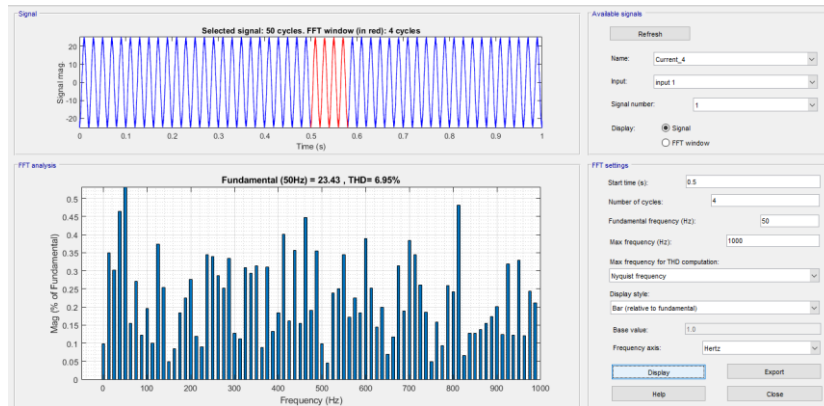
### 3. SIMULATION RESULTS



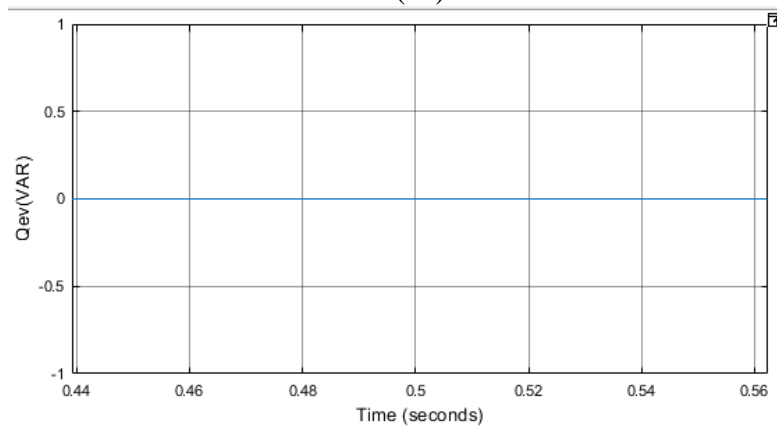
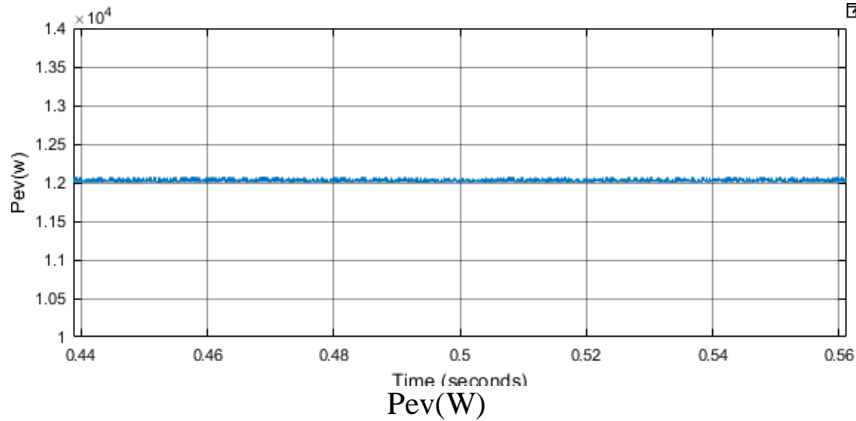
THD of voltage



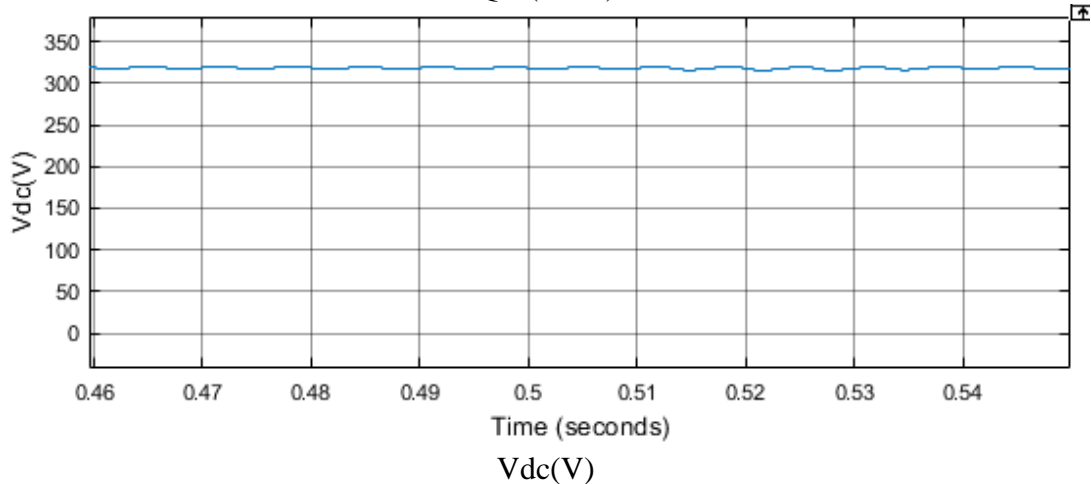
Current



THD of current

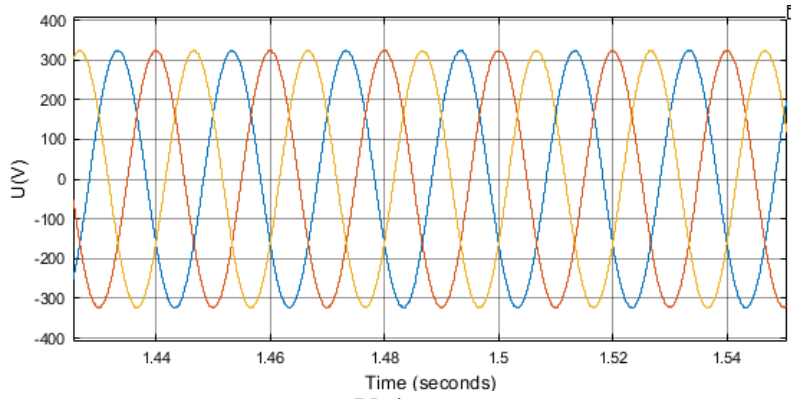


Qev(VAR)

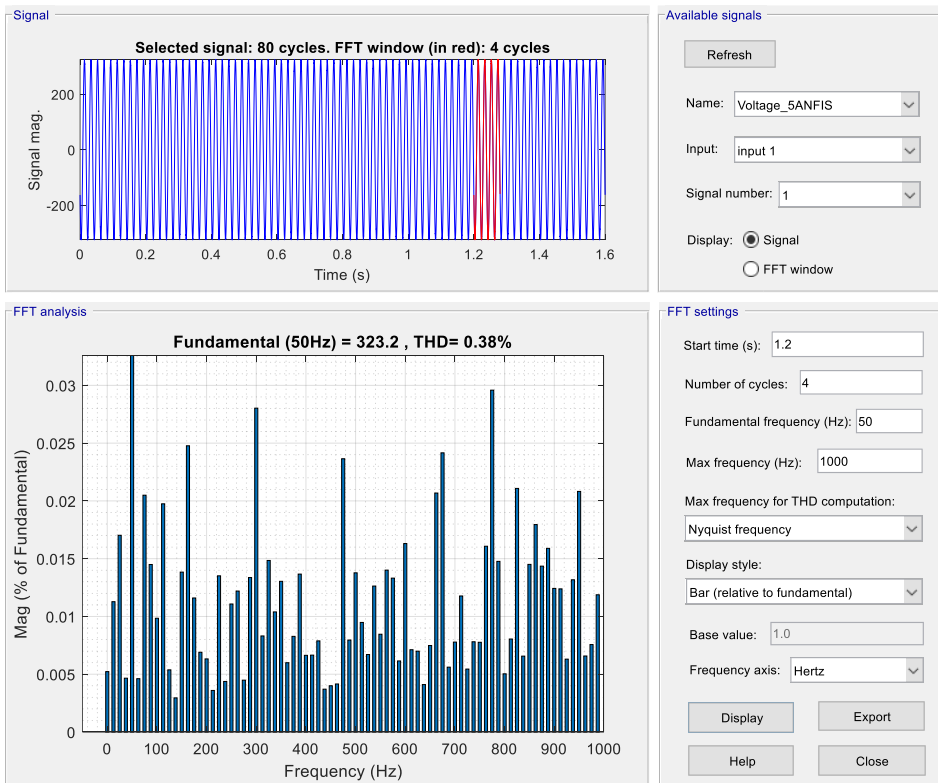


Vdc(V)

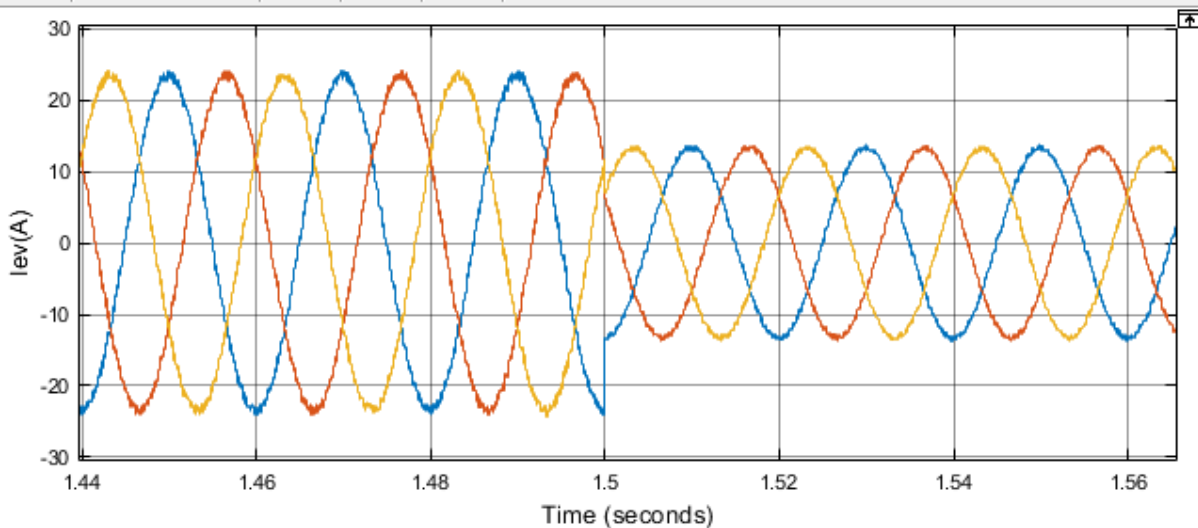
Fig.4



Voltage

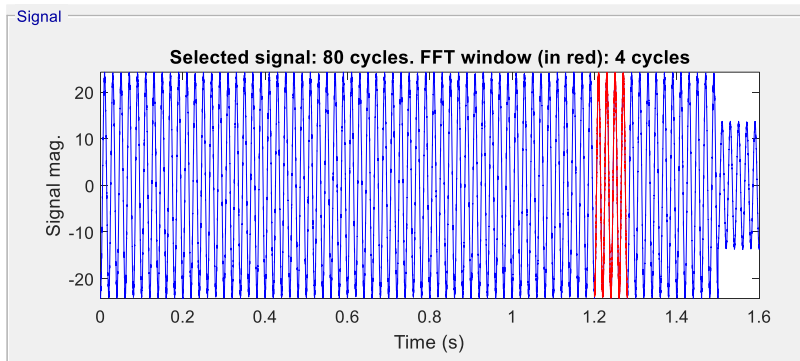


THD of Voltage



Current





Available signals

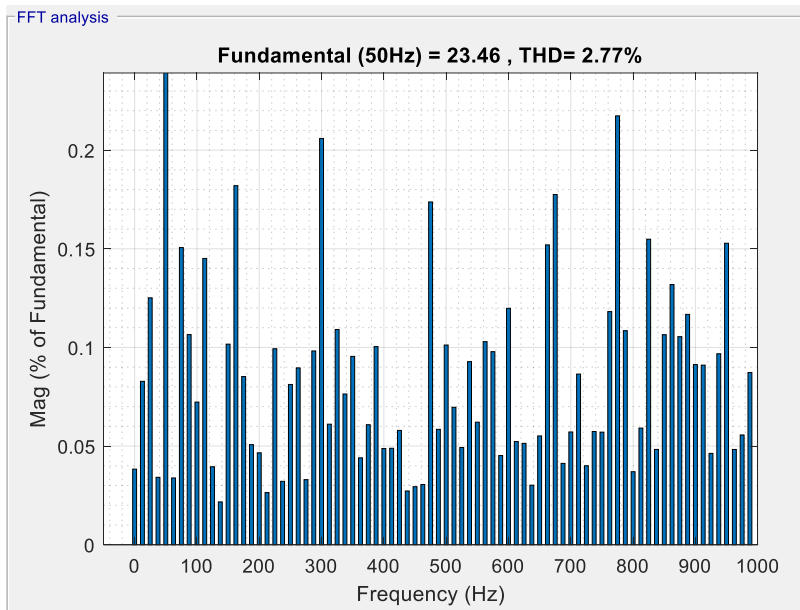
Refresh

Name:

Input:

Signal number:

Display:  Signal  FFT window



FFT settings

Start time (s):

Number of cycles:

Fundamental frequency (Hz):

Max frequency (Hz):

Max frequency for THD computation:

Display style:

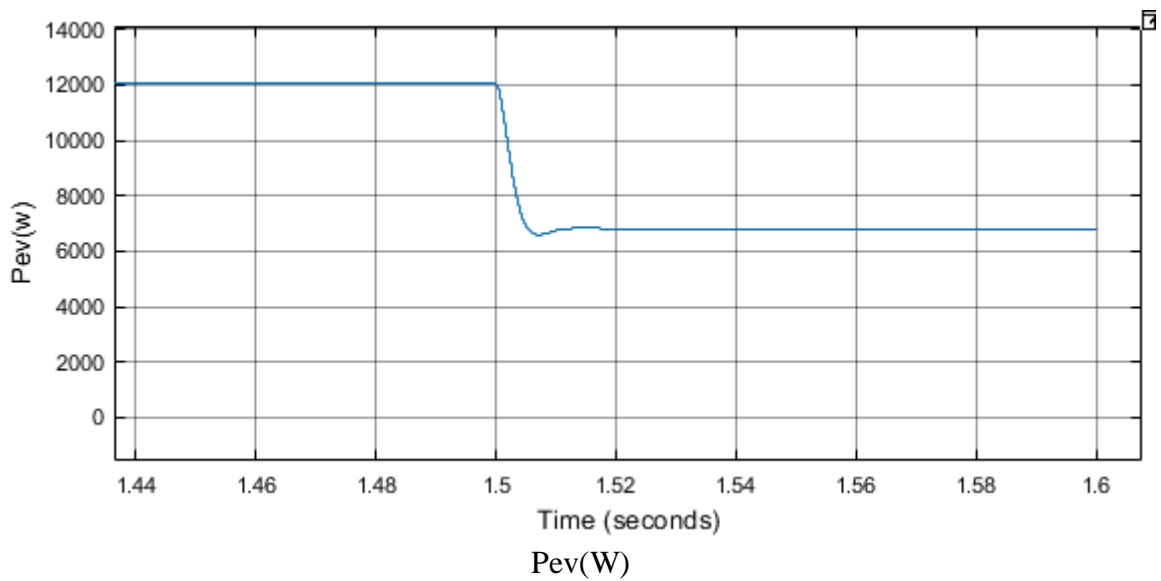
Base value:

Frequency axis:

Display Export

Help Close

THD of current



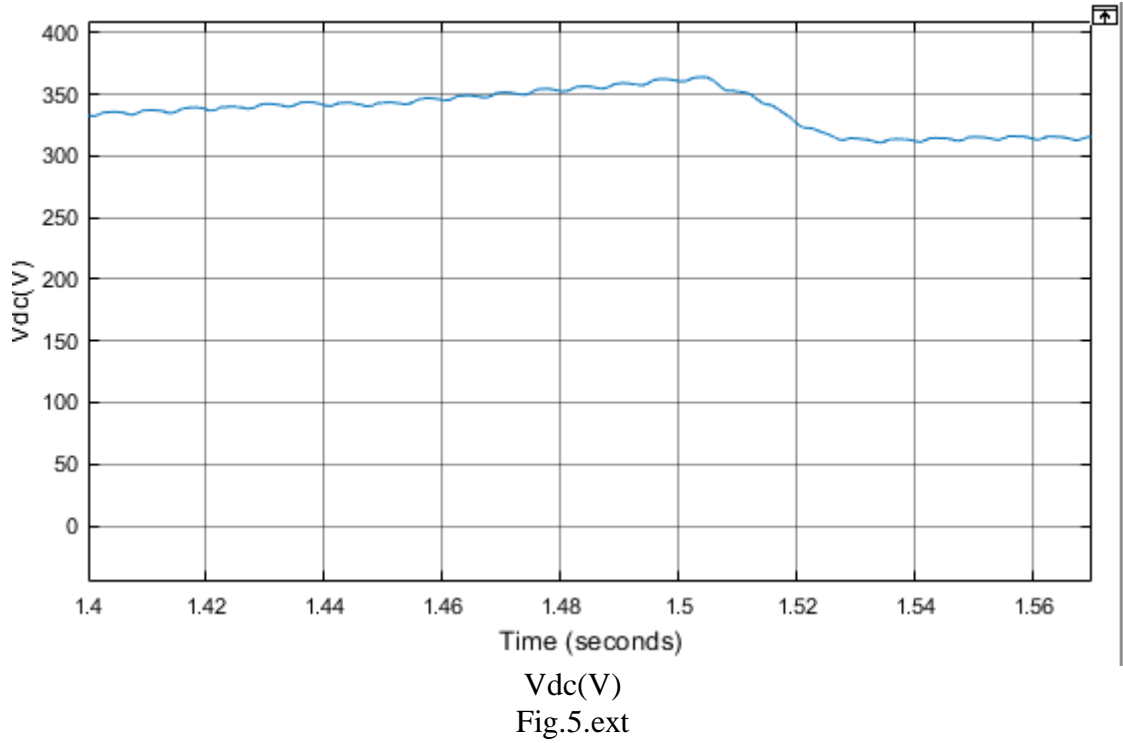
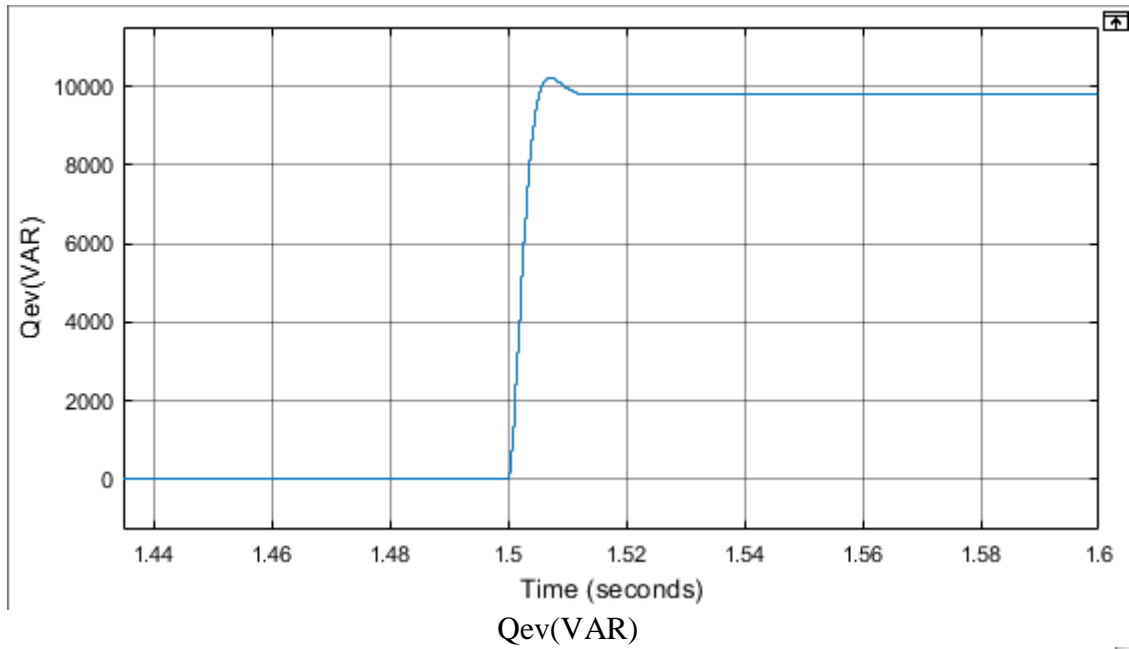
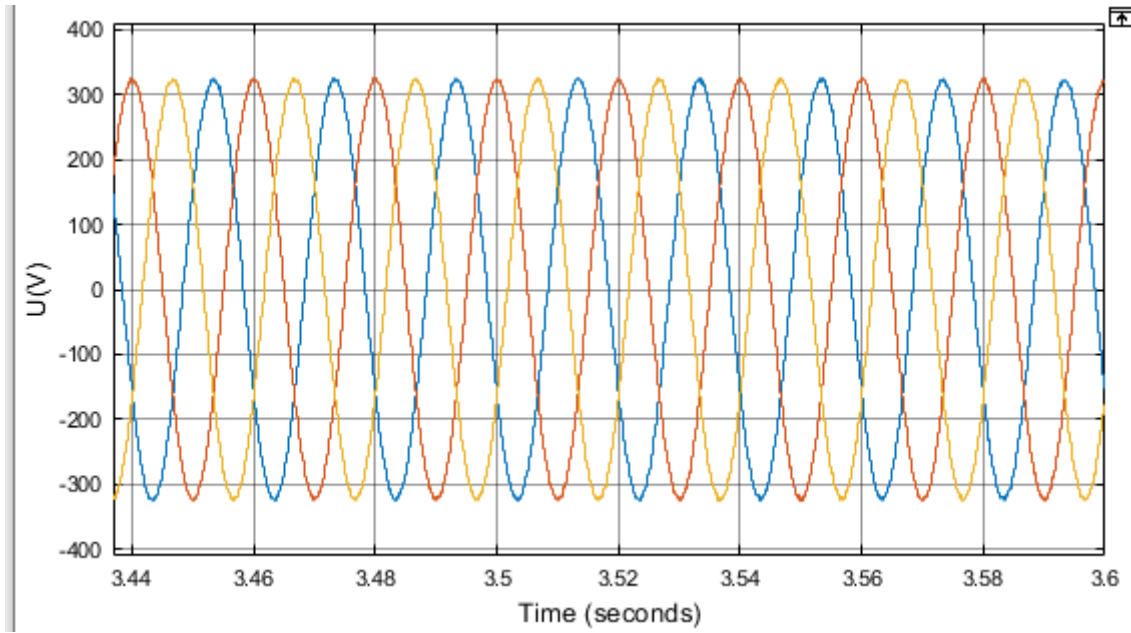


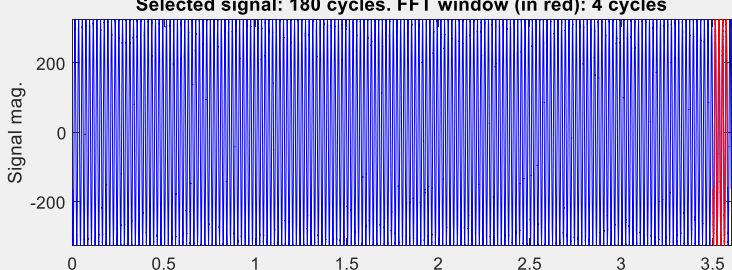
Fig.5.ext



Voltage

Signal

Selected signal: 180 cycles. FFT window (in red): 4 cycles



Signal mag.

Time (s)

Available signals

Refresh

Name: Voltage\_6ANFIS

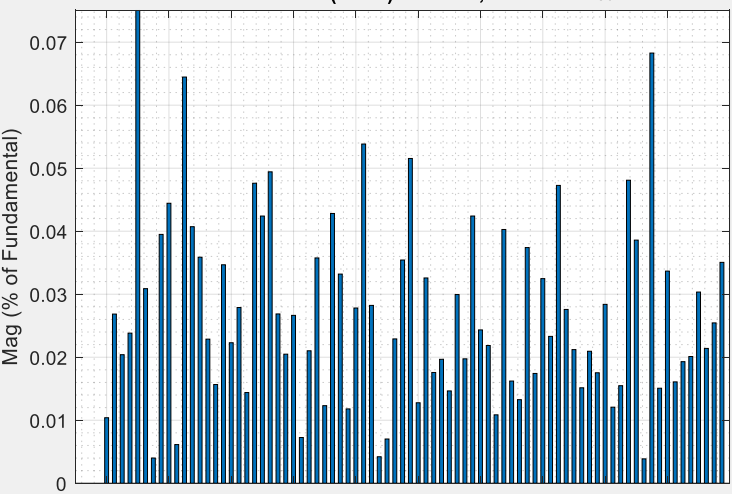
Input: input 1

Signal number: 1

Display:  Signal  FFT window

FFT analysis

Fundamental (50Hz) = 323.2 , THD= 0.76%



Mag (% of Fundamental)

Frequency (Hz)

FFT settings

Start time (s): 3.5

Number of cycles: 4

Fundamental frequency (Hz): 50

Max frequency (Hz): 1000

Max frequency for THD computation: Nyquist frequency

Display style: Bar (relative to fundamental)

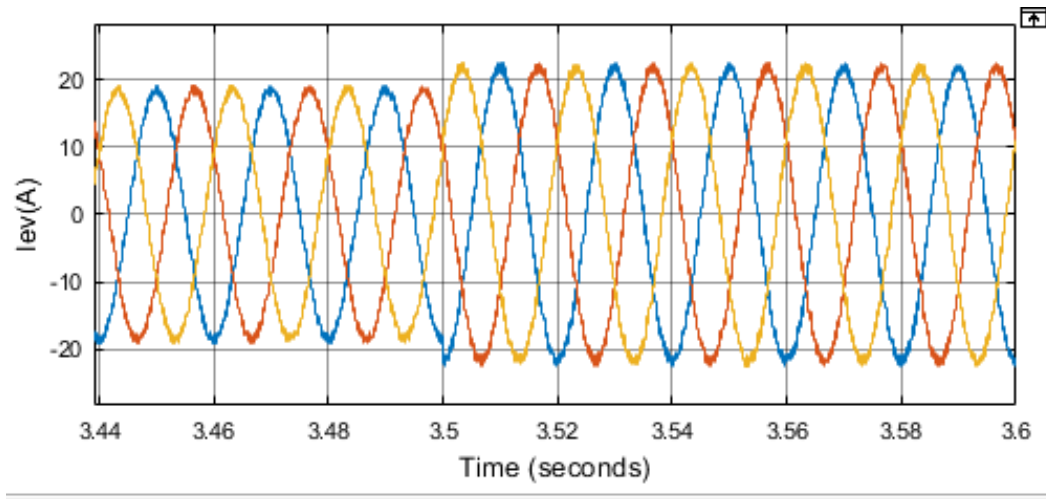
Base value: 1.0

Frequency axis: Hertz

Display Export

Help Close

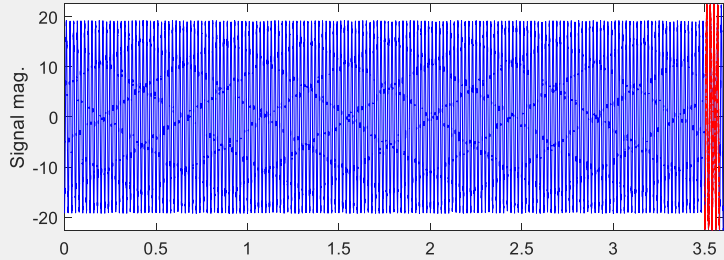
THD of Voltage



Current

Signal

Selected signal: 180 cycles. FFT window (in red): 4 cycles



Signal mag.

Time (s)

Available signals

Refresh

Name: Current\_6ANFIS

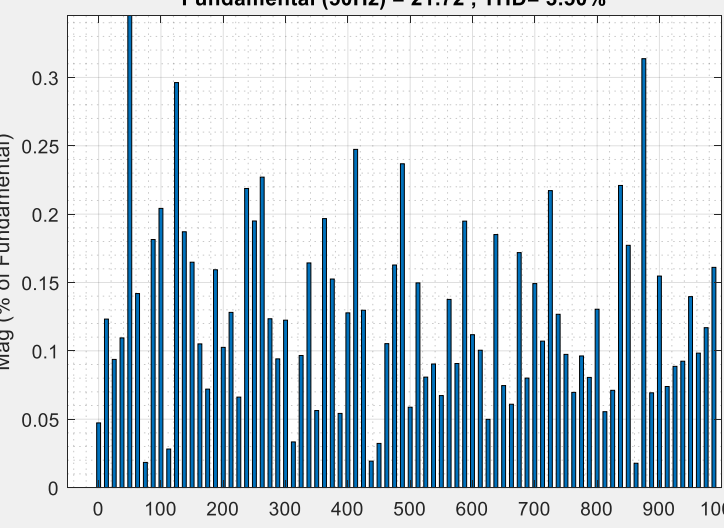
Input: input 1

Signal number: 1

Display:  Signal  FFT window

FFT analysis

Fundamental (50Hz) = 21.72 , THD= 3.50%



Mag (% of Fundamental)

Frequency (Hz)

FFT settings

Start time (s): 3.5

Number of cycles: 4

Fundamental frequency (Hz): 50

Max frequency (Hz): 1000

Max frequency for THD computation: Nyquist frequency

Display style: Bar (relative to fundamental)

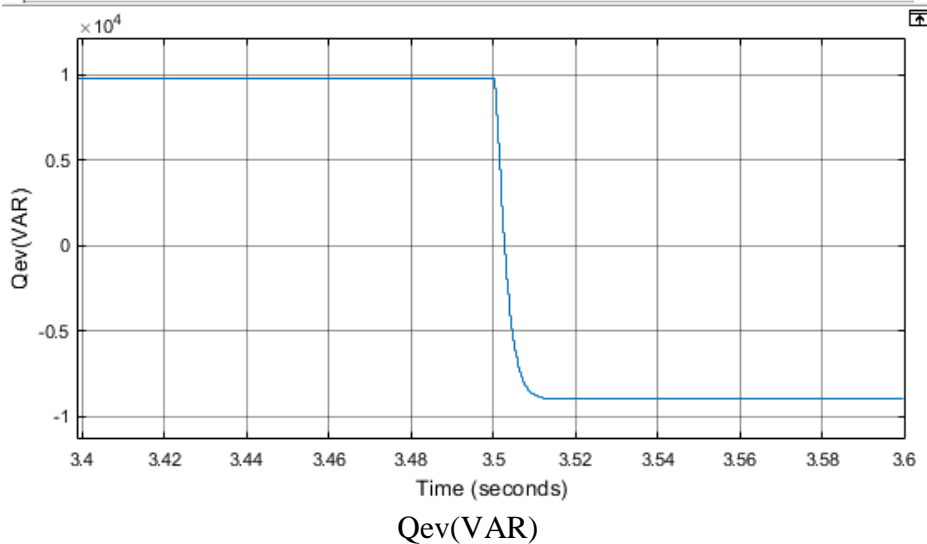
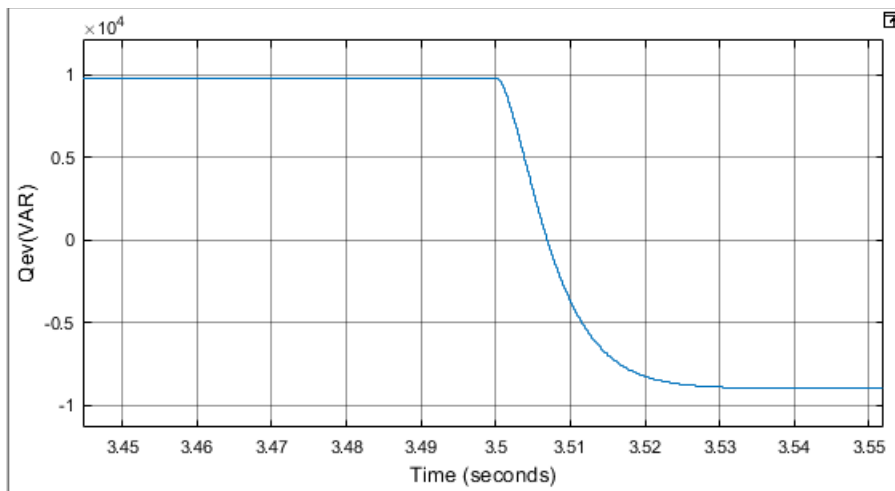
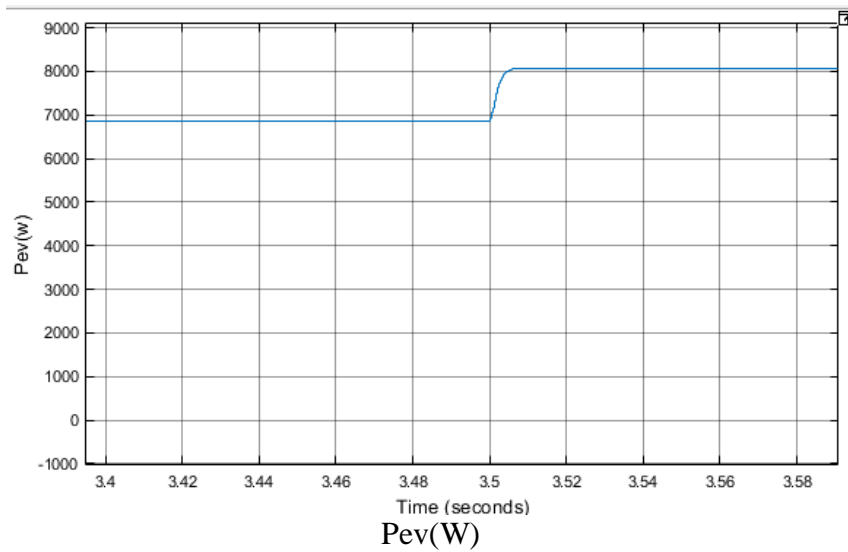
Base value: 1.0

Frequency axis: Hertz

Display Export

Help Close

THD of grid Current



### CONCLUSION

An ANFIS-based effective control system using EVs as an active component that can store, utilise, and provide power is shown in this project, which also addresses G2V and V2G modes as well as reactive power compensation. This project. Galvanic separation on the individual give up is included in the charger configuration for safety reasons. With a little strength practise, the ANFIS-based

complete control rules set works effectively in a variety of working conditions and modes of operation. Consistent-nation and dynamic charging modes work well with the charger. When the electrical command changes, the off-board charger reacts quickly. The EV battery is unaffected by reactive electrical operation, allowing it to last longer. The suggested controller's performance under a variety of strong command conditions has been shown by the simulation results. Findings show that the charger described is a strong competitor for grid power reactive power aid solutions in MATLAB/SIMULINK environments.

## REFERENCES

- [1] S. S. Williamson, A. K. Rathore and F. Musavi, "Industrial Electronics for Electric Transportation: Current State-of-the-Art and Future Challenges," in *IEEE Transactions on Industrial Electronics*, vol. 62, no. 5, pp. 3021-3032, May 2015.
- [2] A. Kuperman, U. Levy, J. Goren, A. Zafransky, and A. Savernin, "Battery charger for electric vehicle traction battery switch station," *IEEE Trans. Ind. Electron.*, vol. 60, no. 12, pp. 5391–5399, 2013.
- [3] M. Restrepo, J. Morris, M. Kazerani and C. A. Cañizares, "Modeling and Testing of a Bidirectional Smart Charger for Distribution System EV Integration," *IEEE Transactions on Smart Grid*, vol. 9, no. 1, pp. 152-162, Jan. 2018.
- [4] A. Khaligh and S. Dusmez, "Comprehensive Topological Analysis of Conductive and Inductive Charging Solutions for Plug-In Electric Vehicles," *IEEE Transactions on Vehicular Technology*, vol. 61, no. 8, pp. 3475-3489, Oct. 2012.
- [5] S. E. Letendre and W. Kempton, "The V2G concept: a new model for power?" *Public Utilities Fortnightly*, pp. 16–26, Feb. 2002.
- [6] M. Yilmaz and P. T. Krein, "Review of the impact of vehicle-to-grid technologies on distribution systems and utility interfaces," *IEEE Trans. Power Electron.*, vol. 28, no. 12, pp. 5573–5689, Dec. 2013.
- [7] M. NikkhahMojdehi and P. Ghosh, "An On-Demand Compensation Function for an EV as a Reactive Power Service Provider," in *IEEE Transactions on Vehicular Technology*, vol. 65, no. 6, pp. 4572-4583, June 2016.
- [8] Buja, M. Bertoluzzo and C. Fontana, "Reactive Power Compensation Capabilities of V2G-Enabled Electric Vehicles," *IEEE Trans, Power Electronics*, vol. 32, no. 12, pp. 9447-9459, Dec. 2017.
- [9] D. B. WickramasingheAbeywardana, P. Acuna, B. Hredzak, R. P. Aguilera and V. G. Agelidis, "Single-Phase Boost Inverter-Based Electric Vehicle Charger With Integrated Vehicle to Grid Reactive Power Compensation," *IEEE Transactions on Power Electronics*, vol. 33, no. 4, pp. 3462-3471, April 2018.
- [10] M. NikkhahMojdehi and P. Ghosh, "An On-Demand Compensation Function for an EV as a Reactive Power Service Provider," *IEEE Trans. Vehicular Technol.*, vol. 65, no. 6, pp. 4572-4583, June 2016.